Microfluid Nanofluid (2005) 1: 208–217
DOI 10.1007/s10404-004-0011-x

RESEARCH PAPER

Zhigang Wu · Nam-Trung Nguyen

Convective–diffusive transport in parallel lamination micromixers

Received: 3 July 2004 / Accepted: 17 September 2004 / Published online: 10 November 2004

Abstract Effective mixing and a controllable concentration gradient are important in microfluidic applications. From the scaling law, decreasing the mixing length can shorten the mixing time and enhance the mixing quality. The small sizes lead to small Reynolds numbers and a laminar flow in microfluidic devices. Under these conditions, molecular diffusion is the main transport effect during the mixing process. In this paper, we present complete 2D analytical models of convective–diffusive transport in parallel lamination micromixers for a binary system. An arbitrary mixing ratio between solute and solvent is considered. The analytical solution indicates the two important parameters for convective–diffusive transport in microchannels: the Peclet number and the dimensionless mixing length. Furthermore, the model can also be extended to the mixing of multiple streams—a common and effective concept of parallel mixing in microchannels. Using laser machining and adhesive bonding, polymeric micromixers were fabricated and tested to verify the analytical results. The experimental results agree well with the analytical models.

Keywords Micromixer · Mass transfer · Diffusion · Parallel lamination · Fluorescent measurement

1 Introduction

Over the past few years, numerous microfluidic devices and systems have been developed for chemical and biochemical applications. Micromixing, as an indispensable process in microfluidic systems, becomes a challenge for the microfluidic community. In most microfluidic devices, the small Reynolds numbers lead to the laminar flow. Thus, conventional methods in the macroscale for enhancing mixing become less effective in the microscale.

A number of works have been carried out on micromixers, which can be categorised as active mixers and passive mixers [1]. The parallel lamination mixer belongs to the passive type. Parallel lamination splits the inlet streams into n substreams, and then joins them into one stream as laminae. The basic design is a long microchannel with two inlets ($n=2$). According its geometry, this design is often called the T-mixer [2, 3] or the Y-mixer [4]. These basic devices lead to the designs of other different passive micromixers [5–8], the discrete droplet mixer [9] and the injection mixer [10]. Mixing can be improved either through increasing the number of contact areas or reducing the mixing path. Furthermore, passive mixers such as the packed-bed mixer [11, 12], the serpentine-shape mixer [13], the grooved patten mixer [14, 15] and the stereo mixer [16, 17] utilise chaotic advection to improve mixing.

In active mixers, external energy is used to affect the flow field and to improve mixing. The external energy can be mechanical [18], acoustic/ultrasonic [19, 20], electrokinetic [21], magnetic [22, 23] or thermal [24]. In general, active mixers have a higher mixing efficiency. However, the requirement of extra energy makes them difficult to be integrated into a microfluidic chip. Furthermore, the relatively high power consumption and cost make active mixers less attractive for disposable applications. Often, passive mixers are preferred.

As mentioned above, many experimental works on micromixers have been done, but little has been reported about mixing theory in micromixers. Ismagilov et al. [25] modelled mixing in microchannels without considering diffusion effect along the flow direction. No analytical solution was given in this work. Later, a similar approach was presented by Kamholz et al. [26]. By introducing an effective dispersion coefficient [27], Beard [28], a later

Z. Wu · N.-T. Nguyen (✉)
School of Mechanical and Production Engineering,
Nanyang Technological University,
50 Nanyang Avenue, 639798, Singapore
E-mail: mntnguyen@ntu.edu.sg
Tel.: +65-6790-4457
Fax: +65-6791-1859

comment [29] and the response [30] simplified the 3D model to a 2D analytical model with the assumption that the channel's width is much larger than its height. However, the analytical form of this solution is very complicated. Further analysis based on this solution seems to be rigorous. This model is not really suitable for the parametric optimisation and evaluation of micromixers. Recently, Holden et al. [31] presented the analytical solution for the 2D mixing model in microchannels without considering the diffusion effect along the flow direction. Our recent work considers the non-linear behaviour of the diffusion process [33]. All of the above works assumed a 1:1 mixing ratio. In practice, other mixing ratios are often needed in microfluidics to achieve a given concentration. To the best of the authors' knowledge, no analytical model exists for diffusive mixing with an arbitrary ratio. Furthermore, no theoretical work was done on diffusive mixing with multiple streams, as reported experimentally in [6] and [8].

In this paper, we present a complete 2D analytical model for diluted convective–diffusive transport in a parallel lamination micromixer with an arbitrary mixing ratio. Based on the simple analytical expression, we found that the dimensionless mixing length is very important for convective–diffusive mixing in microchannels. Furthermore, the solution can be extended to parallel lamination mixing with multiple streams. The theoretical results are validated by experiments. Polymeric micromixers were fabricated using laser micromachining and adhesive bonding. The mixers were characterised using an optical measurement setup.

2 Analytical modelling

The ratio between mass transport due to convection and diffusion is represented by the Peclet number:

$$\mathrm{Pe} = \frac{UW}{D} \tag{1}$$

where U is the average velocity of the stream, W is the channel width and D is the diffusion coefficient. From the definition in Eq. 1, the two influencing factors for convective–diffusive mixing are the velocity distribution across the mixing channel and the diffusion coefficient D. Non-linearities in the concentration distribution may be caused by these two factors. The following analytical models are established for investigating this problem.

2.1 Velocity distribution inside the mixing channel

A simple model for the velocity distribution is based on a parallel mixer with two inlets. The purpose of this model is to investigate the impact of the different viscosities of the fluids. In order to simplify the problem in the microchannel, the two streams are considered as immiscible. This case is acceptable for miscible streams at high Peclet numbers. Previously, Galambos et al. [34] and Stile et al. [35] established a similar model, but no extensive solutions were given. For the model of the channel cross-section depicted in Fig. 1, the fully developed flow in the microchannel is governed by the Navier–Stokes equations:

$$\begin{aligned} \frac{\partial^2 u_1}{\partial y^2} + \frac{\partial^2 u_1}{\partial z^2} &= \frac{1}{\eta_1}\frac{\mathrm{d}p}{\mathrm{d}x} \\ \frac{\partial^2 u_2}{\partial y^2} + \frac{\partial^2 u_2}{\partial z^2} &= \frac{1}{\eta_2}\frac{\mathrm{d}p}{\mathrm{d}x} \end{aligned} \tag{2}$$

where η_1 and η_2 are the viscosities of the two streams and $\mathrm{d}p/\mathrm{d}x$ is the pressure gradient along the x axis. By non-dimensionlising the coordinate system by the channel using W, the dimensionless Navier–Stokes equations for regions 1 and 2 in Fig. 1 are:

$$\begin{aligned} \frac{\partial^2 u_1^*}{\partial y^{*2}} + \frac{\partial^2 u_1^*}{\partial z^{*2}} &= P' \\ \frac{\partial^2 u_2^*}{\partial y^{*2}} + \frac{\partial^2 u_2^*}{\partial z^{*2}} &= \frac{P'}{\beta} \end{aligned} \tag{3}$$

where $P' = W^2/(\eta_1 u_0)\mathrm{d}p/\mathrm{d}x$, representing the constant pressure gradient along the channel with reference velocity u_0 and ratio of viscosities $\beta = \eta_2/\eta_1$. The non-slip conditions at the wall results in:

$$\begin{aligned} u_2^*(1,\ z^*) &= 0 \\ u_1^*(0,\ z^*) &= 0 \end{aligned} \tag{4}$$

At the interface position r between the two streams, the velocity and the shear stress are continuous:

$$\begin{aligned} u_2^*(r,\ z^*) &= u_1^*(r,\ z^*) \\ \left.\frac{\partial u_1^*}{\partial y^*}\right|_{y^*=r} &= \beta \left.\frac{\partial u_2^*}{\partial y^*}\right|_{y^*=r} \end{aligned} \tag{5}$$

For a flat channel ($h^* \ll 1$) and a constant fluid density, the interface position of the two streams can be estimated based on the mass conservation as:

$$r = \frac{1}{1+\beta\gamma} \tag{6}$$

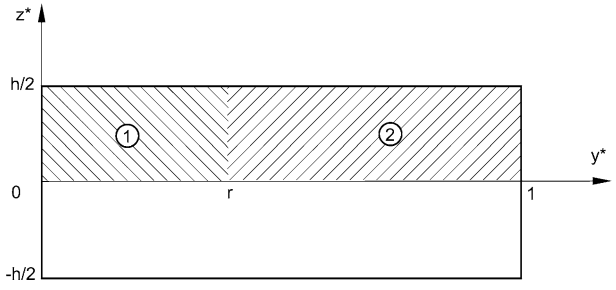

Fig. 1 Dimensionless model of two immiscible streams for estimating the velocity distribution inside the mixing channel. Only half of the channel cross-section (*hatched areas*) is considered in the analytical model

where $\gamma = Q_2/Q_1$ is the ratio of flow rates. Galambos et al. [34] only discussed the special case of $\gamma = 1$. The solutions of Eq. 3 have the Fourier forms ($0 < y^* < 1$, $0 < z^* < h/2$):

$$u_1^*(y^*, z^*) = P'\left[\frac{z^{*2} - h^2/4}{2} + \sum_{n=1}^{\infty} \cos\theta z^* (A_1 \cosh\theta y^* + B_1 \sinh\theta y^*)\right]$$

$$u_2^*(y^*, z^*) = \frac{P'}{\beta}\left[\frac{z^{*2} - h^2/4}{2} + \sum_{n=1}^{\infty} \cos\theta z^* (A_2 \cosh\theta y^* + B_2 \sinh\theta y^*)\right] \quad (7)$$

The coefficients A_1, A_2, B_1 and B_2 can be obtained by solving the Fourier series with the above boundary conditions:

$$A_1 = (-1)^{n+1}\frac{4h^2}{(2n-1)^3\pi^3}$$

$$B_1 = A_1\frac{(1-\beta)(1-\cosh\theta)\sinh^2 r\theta + (1-\beta)\cosh r\theta\cosh\theta + \beta\sinh^2\theta}{(1-\beta)\sinh r\theta\cosh r\theta\cosh\theta - \sinh\theta\left(\cosh^2 r\theta - \beta\sinh^2 r\theta\right)} - A_1\frac{(1-\cosh\theta)\sinh r\theta\sinh\theta\left(\cosh^2 r\theta - \beta\sinh^2 r\theta\right) + \cosh^2 r\theta}{(1-\beta)\sinh r\theta\cosh r\theta\cosh\theta - \sinh\theta\left(\cosh^2 r\theta - \beta\sinh^2 r\theta\right)}$$

$$A_2 = A_1\frac{(1-\beta)\sinh r\theta\cosh r\theta\cosh\theta - \sinh\theta\left(\cosh^2 r\theta - \beta\sinh^2 r\theta\right)}{(1-\beta)\sinh r\theta\cosh r\theta\cosh\theta - \sinh\theta\left(\cosh^2 r\theta - \beta\sinh^2 r\theta\right)} + A_1\frac{-\beta\cosh\theta + (1-\beta)\cosh r\theta\cosh\theta - \beta\sinh^2 r\theta + \cosh^2 r\theta}{(1-\beta)\sinh r\theta\cosh r\theta\cosh\theta - \sinh\theta\left(\cosh^2 r\theta - \beta\sinh^2 r\theta\right)}$$

$$B_2 = A_1\frac{\beta\cosh\theta + (\beta-1)\cosh r\theta\cosh\theta + \beta\sinh^2 r\theta - \cosh^2 r\theta}{(1-\beta)\sinh r\theta\cosh r\theta\cosh\theta - \sinh\theta\left(\cosh^2 r\theta - \beta\sinh^2 r\theta\right)} \quad (8)$$

Figure 2 shows the typical velocity distribution in a rectangular channel for streams with different flow rates. For streams with the same viscosity, the velocity distribution is flat, as shown in Fig. 2a. With the low aspect ratio of the microchannel discussed in this paper ($h^* \ll 1$), a uniform velocity U can be assumed across the channel width.

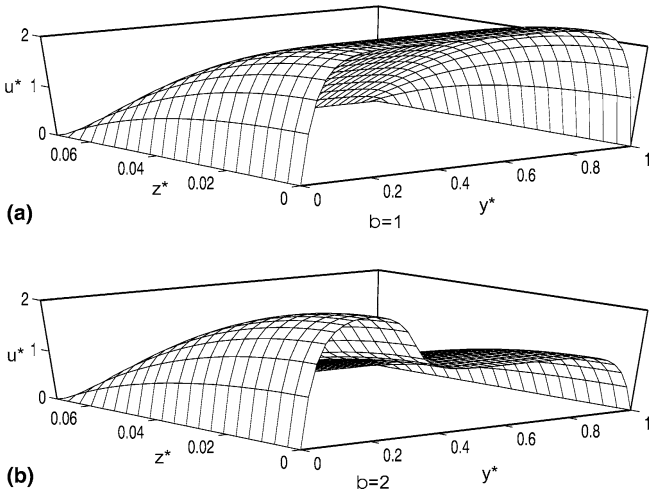

Fig. 2a, b Velocity distribution in a rectangular mixing channel ($h = 0.14$). **a** Same viscosities $\beta = 1$. **b** Different viscosities $\beta = 2$

2.2 Concentration distribution inside the mixing channel

2.2.1 Mixing with two streams

As mentioned in the previous section, for a flat microchannel and mixing streams of the same viscosity, a uniform velocity U across the microchannel can be assumed. Furthermore, no diffusion flux exists in the direction normal to the plane determined by the flow direction and the channel width. This situation appears in a Hele–Shaw-flow or in an electrokinetically driven flow. Thus, the 3D model can be simplified to a 2D model as depicted in Fig. 3. The mixer model consists of a long channel of width W, two inlets and one outlet. One inlet stream is the solute with a concentration of $c = C_0$, the other inlet stream is the solvent with a concentration of $c = 0$. The mass conservation equation including both diffusion and convection can be formulated as [32]:

$$U\frac{\partial c}{\partial x} = D\left(\frac{\partial^2 c}{\partial x^2} + \frac{\partial^2 c}{\partial y^2}\right) \quad (9)$$

where D is the diffusion coefficient of the solute. With the same viscosity ($\beta = 1$) and fluid density, the dimensionless interface location r (Eq. 6) is equal to the mass fraction of the solvent in the final mixture $\alpha = Q_1/(Q_1 + Q_2) = 1/(1+\gamma)$ $(0 \le \alpha \le 1)$. Thus, the mixing ratio of the solute and the solvent is $1{:}\gamma$ or $\alpha{:}(1-\alpha)$. By introducing the dimensionless variables for the coordinates system $x^* = x/W$, $y^* = y/W$, the dimensionless concentration $c^* = c/C_0$ and the Peclet number (from Eq. 1), Eq. 9 has the dimensionless form:

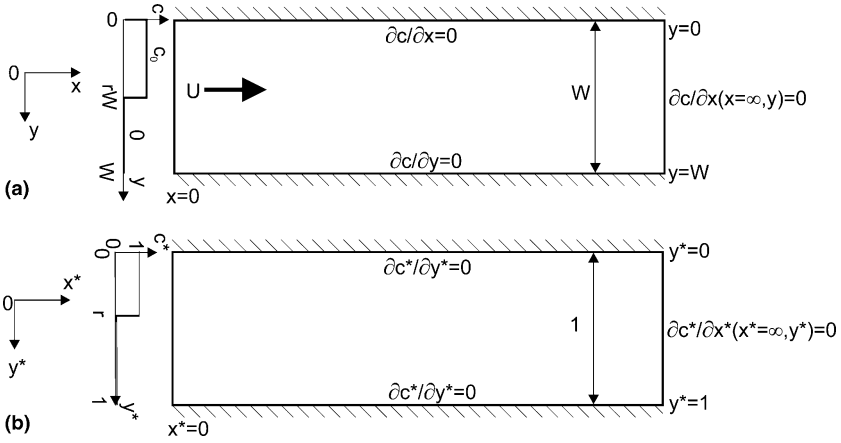

Fig. 3a, b Models for convective–diffusive mixing with an arbitrary mixing ratio in the channels. **a** The physical model. **b** The dimensionless model

$$\mathrm{Pe}\frac{\partial c^*}{\partial x^*} = \frac{\partial^2 c^*}{\partial x^{*2}} + \frac{\partial^2 c^*}{\partial y^{*2}} \tag{10}$$

The corresponding boundary conditions for the inlets are:

$$f(y^*) = \begin{cases} c^*|(x^* = 0,\ 0 \leqslant y^* < r) = 1 \\ c^*|(x^* = 0,\ y^* = r) = 0 \\ c^*|(x^* = 0,\ r < y^* \leqslant 1) = 0 \end{cases} \tag{11}$$

Full mixing is assumed for the outlet, which means:

$$\left.\frac{\partial c^*}{\partial x^*}\right|_{(x^*=\infty,\ 0\leqslant y^*\leqslant 1)} = 0 \tag{12}$$

The channel wall is impermeable. Thus, the flux at the wall should be zero:

$$\left.\frac{\partial c^*}{\partial y^*}\right|_{y^*=0,\ 1} = 0 \tag{13}$$

Equation 13 is also the symmetry condition for mixing with multiple streams, which is discussed later in this section. Equation 10 is a second-order linear partial differential equation. Separating the variables in Eq. 10 and applying the corresponding boundary conditions in Eqs. 11, 12 and 13, the concentration distribution in the channel is:

$$c^*(x^*,\ y^*) = \frac{2}{\pi}\sum_{n=1}^{\infty}\frac{\sin n\alpha\pi}{n}\cos(n\pi y^*) \exp\left(-\frac{2n^2\pi^2}{\mathrm{Pe} + \sqrt{\mathrm{Pe}^2 + 4n^2\pi^2}}x^*\right) + \alpha \quad n = 1,\ 2,\ 3,\ldots \tag{14}$$

Obviously, when $\alpha = 1/2$, resulting in the trivial solution $[0, W]$, the model is the common symmetric (1:1) mixing, as reported previously [33].

2.2.2 Mixing with multiple streams

The above solution can be extended to the case of multiple mixing streams. The trivial solution in Eq. 14 can be extended periodically along the channel width direction. With the distance between two neighbouring concentration extrema $W_{\min,\max}$, the same solution can be extended for micromixers with multiple streams. In this case, the mixing ratio can also be arbitrary. For example, if a ratio of α is given and we let the trivial solution be $[-W_{\min,\max}, W_{\min,\max}]$, an analytical solution for a cross-mixer with three inlets can be obtained using Eq. 14. In this case, the Peclet number is evaluated as $\mathrm{Pe} = UW_{\min,\max}/D$.

Equation 14 consists of three parts: the modulating coefficients, the cosine function and the exponential function. Corresponding to their effects in the expression, the exponential function determines the whole trend of the concentration distribution along flow direction and the cosine function determines the variation in the channel width. If rapid mixing is needed, the absolute value of the exponent should be large. This means that a small Peclet number causes better mixing. Therefore, the Peclet number (Pe) is the most important parameter for the mixing process in parallel lamination micromixers. Figure 4 shows the results of the above analytical model for some typical cases.

3 Experiments

3.1 Materials and methods

Fully polymeric micromixers made of polymethylmethacrylate (PMMA) and acrylic double-layer adhesive tape were used for verifying the theory. The fabrication is based on the laser machining and adhesive lamination technique. The size of the device is 25×75 mm. Basically, the micromixers consist of three layers: the top layer (PMMA) for optical access, the intermediate adhesive layer (Adhesives Research, Inc., Arclad 8102 transfer adhesive) for channel structure and the bottom layer (PMMA) for fluidic access and alignment. First, the three layers were cut using a CO_2 laser with a characteristic wavelength of 10.6 μm. Alignment holes are fabricated in the three layers. On the bottom layer, position marks are ablated for the convenience of later measurements. The three layers are laminated using

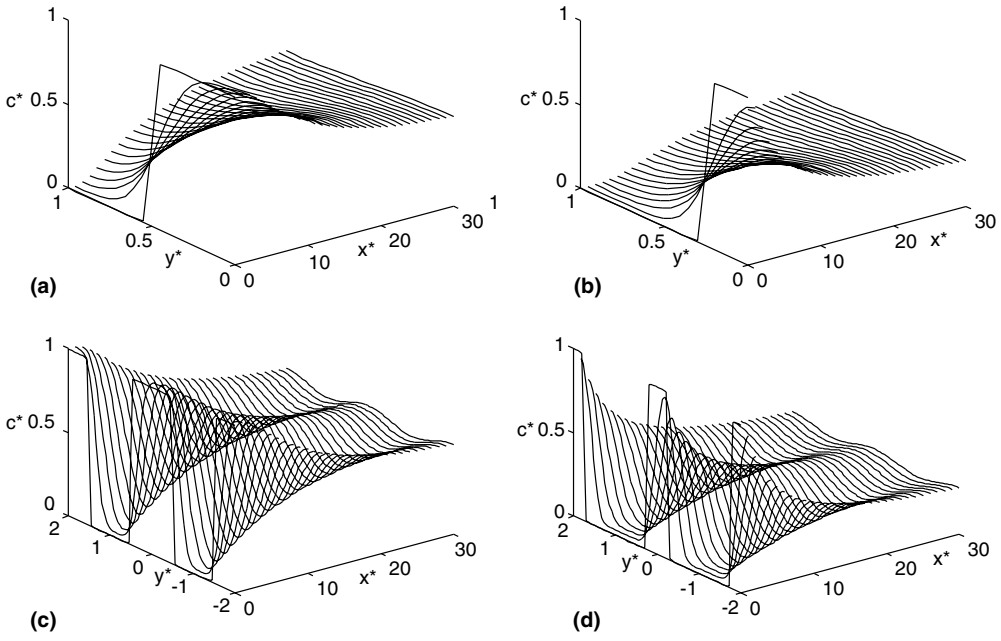

Fig. 4a–d Typical results of the analytical model for Pe = 100. **a** Two streams, mixing ratio 1:1. **b** Two streams, mixing ratio 1:3. **c** Multiple streams, mixing ratio 1:1. **d** Multiple streams, mixing ratio 1:3

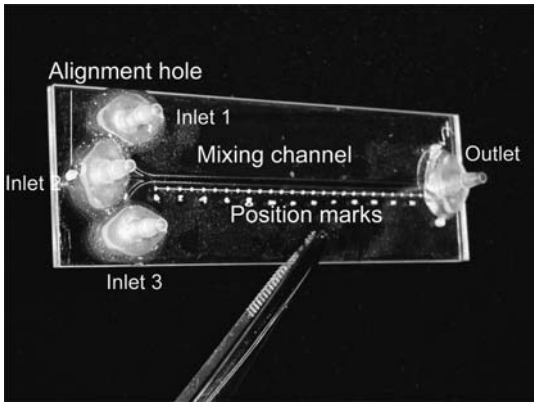

Fig. 5 Polymeric micromixer with three inlets for the experiments

alignment holes. The adhesive layer thickness of 50 μm defines the channel height. Using this technique, a mixing channel of 900 μm in width and 50 μm in height was fabricated for the experiments described in the next sections. This setup is shown in Fig. 5. The resulting aspect ratio of the channel is $h^* \approx 0.056$.

The same image acquisition system as reported in [33] (Fig. 6) was used to measure the velocity distribution and concentration distribution in the mixer. The system consists of three main components: an illumination system (a Mercury lamp and a laser system), an optical system (inverted microscope and CCD camera) and an image acquisition system together with its corresponding software. The laser was used for micro particle image velocimetry (micro-PIV) to verify the uniform velocity distribution in the channels. The two light sources are selected by an optical switch consisting of a reflection mirror. When the mirror is parallel to the input light axis, the laser is active. When the mirror is turned 45° to the inlet axis, the light from the Mercury lamp is active.

Both the micro-PIV and the concentration measurements are based on the fluorescent technique. In the micro-PIV measurement, 3-μm red particles (Duke Scientific Co.) were used to trace the movement of the fluid in the channel. In the concentration measurement, a fluorescent dye was used ($C_{20}H_{10}Na_2O_5$). To enhance the emission light of the fluorescein, 10× TBE buffer (for 1 l 108 g Tris base, Tris (hydroxymethyl)-aminomethane, 55 g Boric acid, and 40 ml 0.5 M ethylene diamine tetraacetic acid (pH 8.0) autoclave for 20 min) was added to the dye solution. The separated fluorescent bands of the microspheres (540/610 nm) and of the dye (490/520 nm) allow the measurements of both the velocity field and the concentration field using the same prepared liquids.

3.2 Results and discussion

3.2.1 Velocity distribution

The PIV measurement uses an epi-fluorescent attachment of type Nikon G-2E/C (excitation filter for 540 nm, dichroic mirror for 565 nm and an emission filter for 605 nm). Both filters in the attachment have a bandwidth of 25 nm.

The measurement reported in this paper was carried out with a 4× objective. With a CCD sensor size of 6.3× 4.8 mm and a resolution of 640×480 pixels, the size of an image pixel is 2.475 μm and the size of the measured area is 1,584×1,188 μm. Two 30-mJ laser pulses with a delay time of 3.5 ms were used as the illumination sources. The integration area is 32×32 pixels.

The velocity measurements were carried out for two cases; water/water and water/diluted glycerol. Diluted

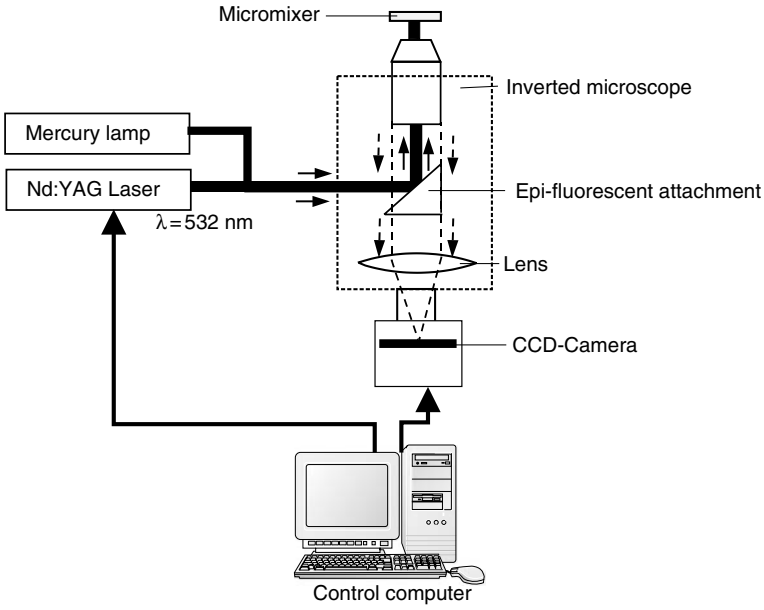

Fig. 6 Optical setup for the fluorescent measurements

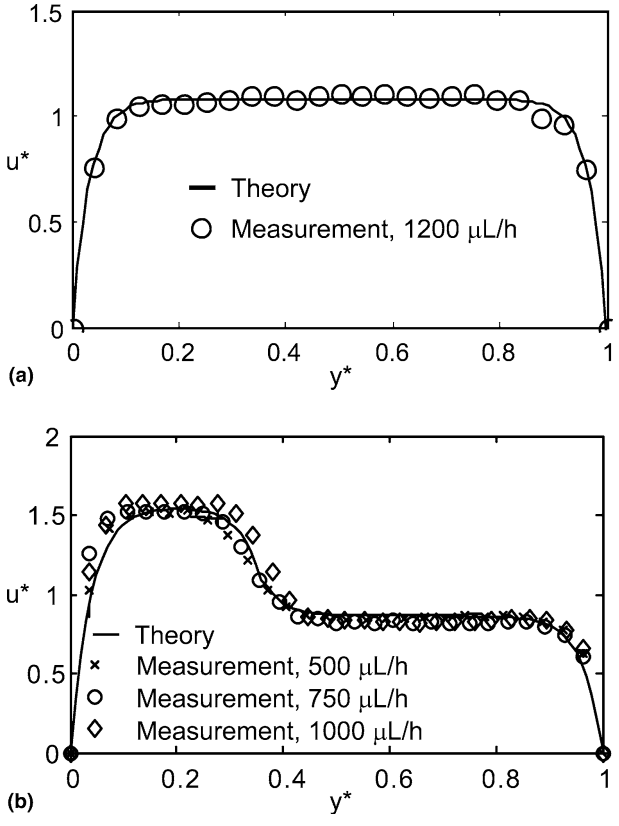

Fig. 7a, b Micro-PIV results for the dimensionless velocity distribution at $x^* = 11.1$. **a** Dimensionless velocity profile with the same viscosity. **b** Dimensionless velocity profile with different viscosities (analytical results are calculated with $\beta = 1.8$)

glycerol with a volume ratio of 1:4 (glycerol to DI-water at 25°C) was used as the fluid with the high viscosity. Measurement of the two liquids with a viscometer (Brookfield LVDV-I) results in a ratio of $\beta = 1.7 \pm 0.2$. Only two inlets of the device were in use. Syringe pumps with identical syringes were used so that the same volumetric flow rate can be assumed for each inlet stream. Figure 7 shows the typical results of the micro-PIV measurement. The influence of the viscosity on the velocity distribution can be seen clearly. The measurement results also validates the assumption of a uniform velocity profile in the case of mixing water with dyed water.

3.2.2 Concentration distribution

In our experiments, a single mixer (Fig. 5) and the same mixing ratio 2:1 were used for both mixing cases. Three identical syringes (Hamintol, 500 μl, gas tight) were used in the experiments: one was filled with deionised (DI-)water and the other two were filled with fluorescent dye diluted in water. For the case of two streams mixing, the syringe with DI-water was connected to inlet 1 and the other two syringes were connected to inlet 2 and inlet 3. For three streams mixing, the syringe with DI-water was connected to inlet 2 and the other two syringes were connected to inlet 1 and inlet 3. All three syringes were driven by a single syringe pump (Cole-Parmer 74900-05, 0.2 μl/h–500 ml/h, accuracy of 0.5%).

With the same mean velocity in the mixing channel, the Peclet number of the latter case was half of the former, due to the smaller mixing length of $W/2$. After successfully finding good agreement between our theory and the experimental results using the two streams case, the same parameters with half of the original Peclet number were applied to fit the results of the three streams mixing.

After recording the images on the computer, the concentration profiles were evaluated using a customised program written in Matlab. First, the program removes the noise in the measured image with an adaptive noise-removal filter. For each pixel, a local mean value is calculated for a window of 5×5 pixels. The noise is assumed

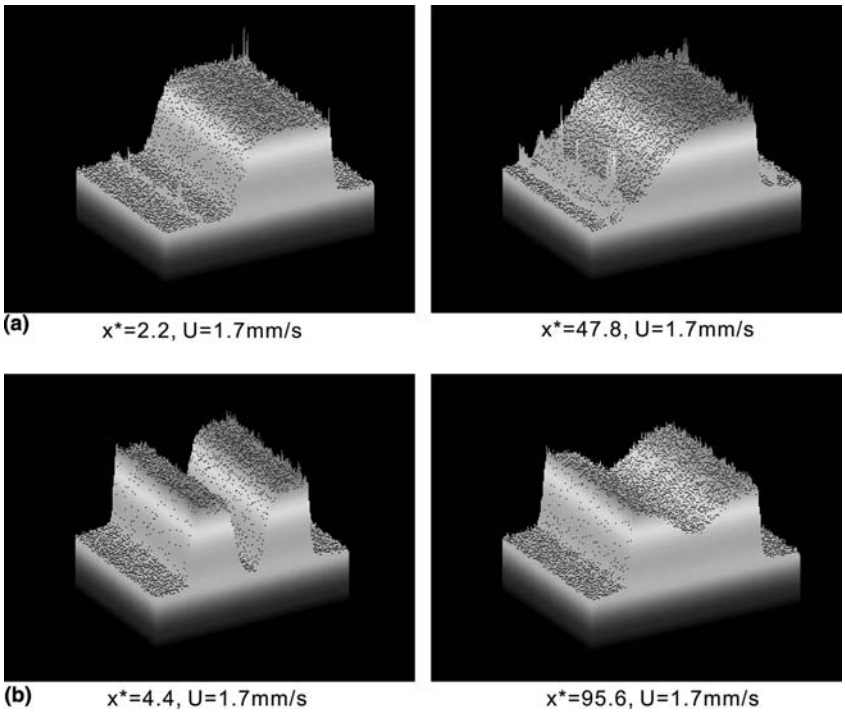

Fig. 8a, b Three-dimensional intensity distribution in the captured image with $U = 1.7$ mm/s and solute/solvent ratio of 2:1 at different positions. **a** Two streams mixing. **b** Three streams mixing

to have a Gaussian distribution. Subsequently, a path with the known position across the channel is evaluated. The position across the channel was normalised against the channel width $y^* = y/W$, while the measured pixel intensity I was normalised against the maximum $I_{\max}$ and minimum $I_{\min}$ of the intensity at the inlet:

$$I^* = \frac{I - I_{\min}}{I_{\max} - I_{\min}} \tag{15}$$

The measured dimensionless intensity is assumed to be equal to the dimensionless concentration of the fluorescent dye ($I^* = c^*$). Figure 8 shows the typical 3D intensity distribution in the mixing channel.

During the evaluation of the results, we observed non-linearity in the concentration distribution. Since the velocity is uniform, the non-linearity can only be caused by the diffusion coefficient D. This effect has already been reported in [36, 37, 38] and analysed in our previous work [33]. The concentration-dependent diffusion coefficient can assume the model:

$$D(c) = D_0\left[(1-a)\frac{c}{c_0} + a\right] \tag{16}$$

where D_0 is the coefficient at the maximum concentration c_0 and a is the factor describing the interaction between the solute and solvent. Since Eq. 16 makes the governing equation in Eq. 10 non-linear, and no pure analytical solution exists for this case, thus, an approximation with the linear solution (Eq. 14) was used to fit the measurement results. The fitting parameters are D_0 and a [33].

Because of both the unknown diffusion coefficient D_0 and the factor a, the non-linear mixing theory was used for fitting the measurement results. While the solute side was used for finding D_0, the solvent side was used for determining the factor a. Using several measurements at different average velocities, the fitting parameters $a = 0.5$ and $D_0 = 1.8\times10^{-9}$ m^2/s could be found for the experiments presented in this paper. Due to the added 10× TBE buffer, these parameters are slightly different to our previous results in [33].

Figures 9 and 10 depict the results of two streams mixing, while Figs. 11 and 12 show the results of three streams mixing. All these figures compare the measured concentration profiles and concentration gradient profiles with the theoretical results using the fitting parameters mentioned above. It can be seen clearly that the non-linear approximation describes relatively well the diffusive mixing process in the microchannel. The broadening band can be observed with the gradient profile. The band is thinner at a higher Peclet number.

During the course of the evaluation, another important parameter was found for the Y-mixer. Ignoring the diffusion in the flow direction, the analytical solution becomes:

$$c^*(x^*,\ y^*) = \frac{2}{\pi}\sum_{n=1}^{\infty}\frac{\sin n\alpha\pi}{n}\cos(n\pi y^*)\exp\left(-\frac{n^2\pi^2}{\mathrm{Pe}}x^*\right) + \alpha$$
$$n = 1,\ 2,\ 3,\ldots \tag{17}$$

In [31], from the expression of the exponent (similar to the exponent in Eq. 17), Holden et al. introduced a dimensionless parameter $\kappa = x^*/\mathrm{Pe}$. However, they did not give any further explanation on it. In our opinion, this parameter can be regarded as a dimensionless mixing length in microchannels. If the channel length is L, the residence time is $t = L/U$. According to Einstein [39],

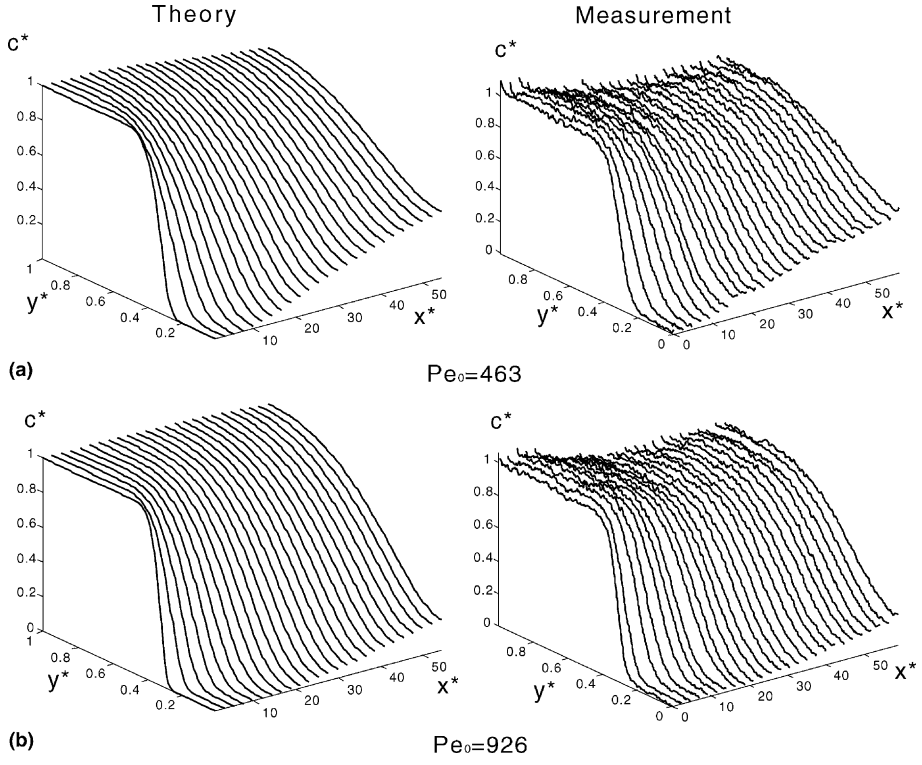

Fig. 9a, b Dimensionless concentration distribution for two streams mixing (2:1 ratio) in the channels. **a** $Pe_0 = 463$. **b** $Pe_0 = 926$

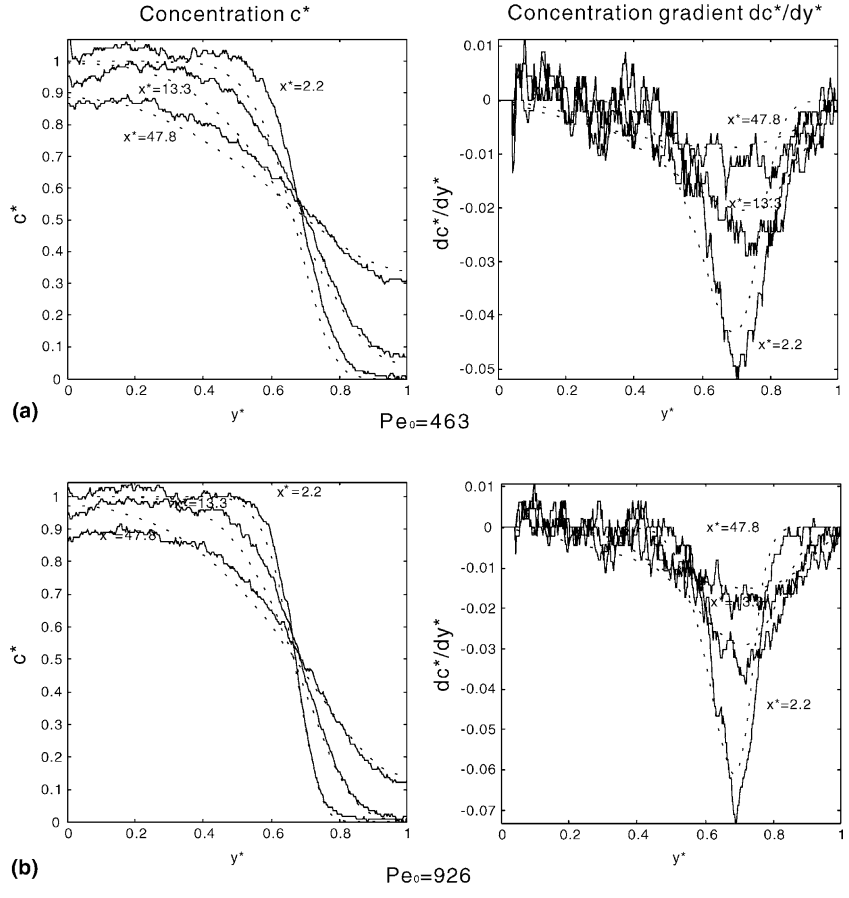

Fig. 10a, b Distribution of concentration and concentration gradient across the channel at $x^* = 2.2$, $x^* = 13.3$ and $x^* = 47.8$ for three streams mixing (ratio is 2:1) (*solid lines* are measured results, *dashed lines* are theoretical results with $D_0 = 1.8 \times 10^{-9}$ and $a = 0.5$). **a** $Pe_0 = 463$. **b** $Pe_0 = 926$

t is proportional to W^2/D. Thus, L is proportional to UW^2/D. Dividing x by UW^2/D results in the proportionality factor $DL/UW^2 = x^*/\mathrm{Pe}$. In system theory, the response function $\exp(-t/\tau)$ is considered complete when $t \approx 3\tau$. Similar to this approach, κ can be used for judging whether or not good mixing is obtained.

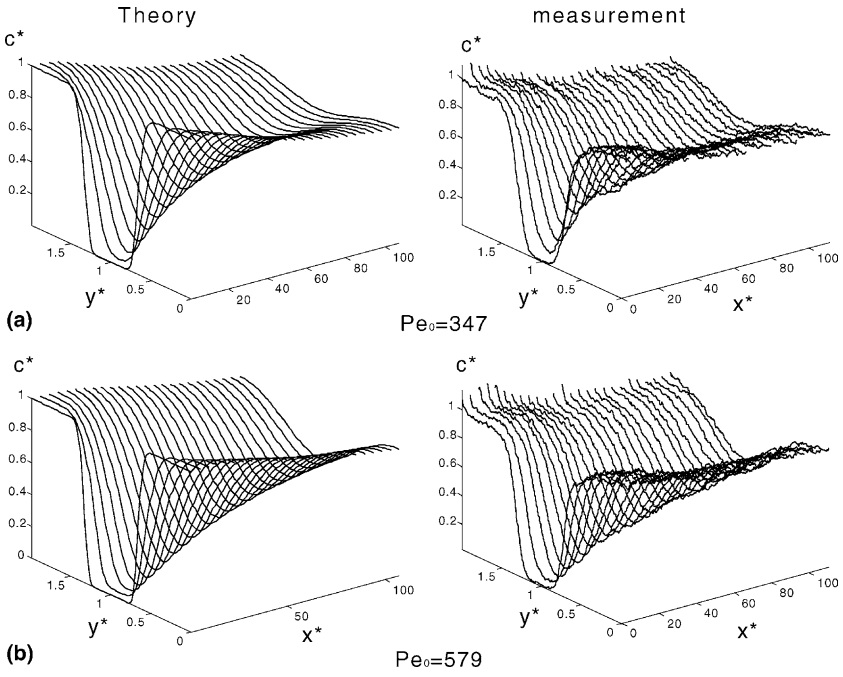

Fig. 11a, b Dimensionless concentration distribution for asymmetric (ratio is 2:1) multiple mixing in the channels. **a** $Pe_0 = 347$. **b** $Pe_0 = 579$

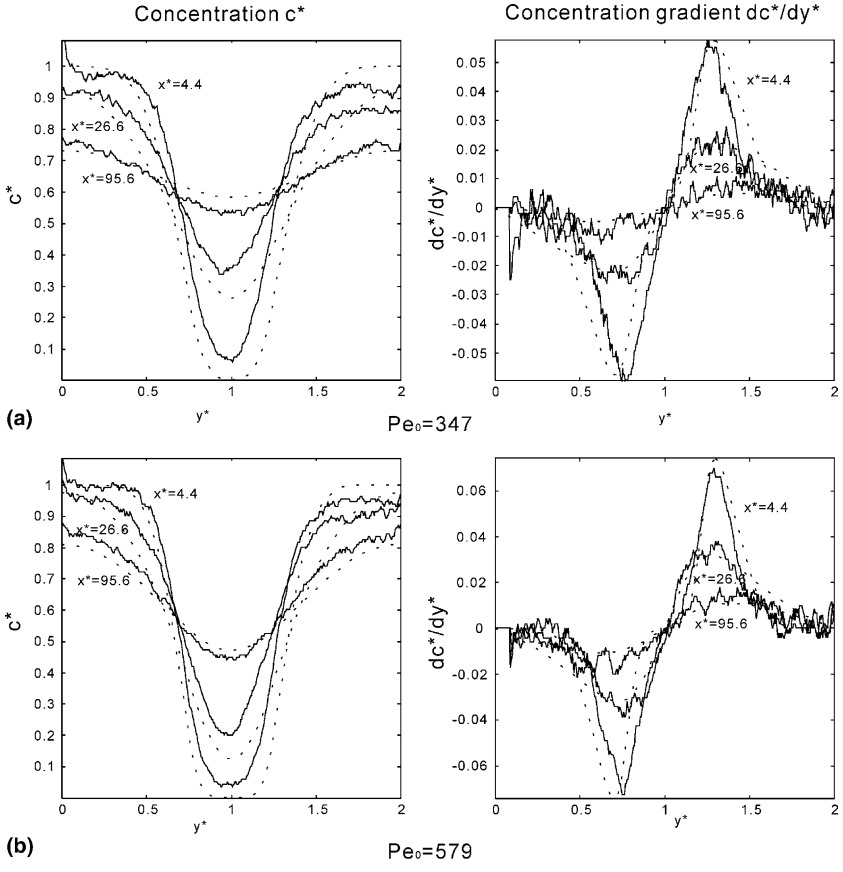

Fig. 12 Distribution of concentration and concentration gradient for asymmetric (ratio is 2:1) multiple mixing across the channel at $x^* = 4.4$, $x^* = 26.6$ and $x^* = 95.6$ (*solid lines* are measured results, *dashed lines* are theoretical results with $D_0 = 1.8 \times 10^{-9}$ and $a = 0.5$). **a** $Pe_0 = 347$. **b** $Pe_0 = 579$

3.3 Conclusions

Two-dimensional analytical models for the velocity distribution and diluted convective–diffusive mixing in parallel lamination micromixers with an arbitrary mixing ratio were presented in this paper. All the previously reported models are special cases of this new analytical model. Furthermore, the solution can be applied for parallel lamination micromixers with multiple streams because of the similarity of the boundary conditions at the

wall and the symmetry condition in the middle of a single stream. We demonstrated that the Peclet number and the dimensionless mixing length κ are the most important parameters for a passive T-mixer. All these conclusions were verified by the experimental results. The model presented in the paper can be used as an analytical tool for the parametric optimisation of passive micromixers.

Acknowledgements This work was supported by the academic research fund of the Ministry of Education Singapore, contract number RG11/02. The first author wishes to gratefully acknowledge the PhD scholarship from Nanyang Technological University.

References

1. Nguyen NT, Wereley ST (2003) Fundamentals and applications of microfluidics. Artech House, Boston, Massachusetts
2. Kamholz AE, Weigl BH, Finlayson BA, Yager P (1999) Quantitative analysis of molecular interaction in a microfluidic channel: the T-sensor. Anal Chem 71:5340–5347
3. Koch M, Chatelain D, Evans AGR, Brunnschweiler A (1998) Two simple micromixers based on silicon. J Micromech Microeng 8:123–126
4. Gobby D, Angeli P, Gavriilidis A (2001) Mixing characteristics of T-type microfluidic mixers. J Micromech Microeng 11:126–132
5. Ehrfeld W, Golbig K, Hessel V, Löwe H, Richter T (1999) Characterization of mixing in micromixers by a test reaction: single mixing units and mixing arrays. Ind Eng Chem Res 38:1075–1082
6. Erbacher C, Bessoth FG, Busch M, Verpoorte E, Manz A (1999) Towards integrated continuous-flow chemical reactors. Mikrochim Acta 131:19–24
7. Schwesinger N, Frank T, Wurmus H (1996) A modular microfluid system with an integrated micromixer. J Micromech Microeng 6:99–102
8. Koch M, Witt H, Evans G, Brunnschweiler A (1999) Improved characterization technique for micromixers. J Micromech Microeng 9:156–158
9. Handique K, Burns MA (2001) Mathematical modeling of drop mixing in a slit-type microchannel. J Micromech Microeng 11:548–554
10. Miyake R, Lammerink TSJ, Elwenspoek M, Fluitman JHJ (1993) Micro mixer with fast diffusion. In: Proceedings of the 6th IEEE international workshop on micro electro mechanical systems (MEMS'93), Fort Lauderdale, Florida, February 1993, pp 248–253
11. He B, Burke BJ, Zhang X, Zhang R, Regnier FE (2001) A picoliter-volume mixer for microfluidic analytical systems. Anal Chem 73:1942–1947
12. Lin Y, Gerfen GJ, Rousseau DL, Yeh SR (2003) Ultrafast microfluidic mixer and freeze-quenching device. Anal Chem 75:5381–5386
13. Liu RH, Stremler MA, Sharp KV, Olsen MG, Santiago JG, Adrian RJ, Aref H, Beebe DJ (2000) Passive mixing in a three-dimensional serpentine microchannel. J Microelectromech Syst 9:190–197
14. Stroock AD, Dertinger SK, Ajdari A, Mezic I, Stone HA, Whitesides GM (2002) Chaotic mixer for microchannels. Science 295:647–650
15. Wang H, Iovenitti P, Harvey E, Masood S (2003) Numerical investigation of mixing in microchannels with patterned grooves. J Micromech Microeng 13:801–808
16. Bertsch A, Heimgartner S, Cousseau P, Renaud P (2001) Static micromixers based on large-scale industrial mixer geometry. Lab Chip 1:56–60
17. Park SJ, Kim JK, Park J, Chung S, Chung C, Chang JK (2004) Rapid three-dimensional passive rotation micromixer using the breakup process. J Micromech Microeng 14:6–14
18. Evans J, Liepmann D, Pisano AP (1997) Planar laminar mixer. In: Proceeding of the 10th IEEE international workshop on micro electro mechanical systems (MEMS'97), Nagoya, Japan, January 1997, pp 96–101
19. Liu H, Lenigk R, Druyor-Sanchez RL, Yang J, Grodzinski P (2003) Hybridization enhancement using cavitation microstreaming. Anal Chem 75:1911–1917
20. Yang Z, Goto H, Matsumoto M, Maeda R (2001) Ultrasonic micromixer for microfluidic systems. Sensor Actuat A–Phys 93:266–272
21. Oddy MH, Santiago JG, Mikkelsen JC (2001) Electrokinetic instability micromixing. Anal Chem 73:5822–5832
22. Bao HH, Zhong J, Yi M (2001) A minute magneto hydro dynamic (MHD) mixer. Sensor Actuat B–Chem 79:207–215
23. Lu LH, Ryu K, Liu C (2002) A magnetic microstirrer and array for microfluidic mixing. J Microelectromech Syst 11:462–469
24. Tsai JH, Lin L (2002) Active microfluidic mixer and gas bubble filter driven by thermal bubble micropump. Sensor Actuat A–Phys 97–98:665–671
25. Ismagilov RF, Stroock AD, Kenis PJA, Whitesides G, Stone HA (2000) Experimental and theoretical scaling laws for transverse diffusive broadening in two-phase laminar flows in microchannels. Appl Phys Lett 76:2376–2378
26. Kamholz AE, Yager P (2002) Molecular diffusive scaling laws in pressure-driven microfluidic channels: deviation from one-dimensional Einstein approximations. Sensor Actuat B–Chem 82:117–121
27. Brenner H, Edwards DA (1993) Macrotransport processes. Butterworth-Heinemann, Boston, Massachusetts
28. Berad DA (2001) Taylor dispersion of a solute in a microfluidic channel. J Appl Phys 89:4467–4469
29. Dorfman KD, Brenner H (2001) Comment on "Taylor dispersion of a solute in a microfluidic channel." J Appl Phys 90:6553–6554
30. Beard DA (2001) Response to "Comment on "Taylor dispersion of a solute in a microfluidic channel" [J Appl Phys 90:6553]". J Appl Phys 90:6555–6556
31. Holden MA, Kumar S, Castellana E, Beskok A, Cremer PS (2003) Generating fixed concentration arrays in a microfluidic device. Sensor Actuat B–Chem 92:199–207
32. Cussler EL (1984) Diffusion: mass transfer in fluid systems. Cambridge University Press, New York
33. Wu ZG, Nguyen NT, Huang XY (2004) Nonlinear diffusive mixing in microchannels: theory and experiments. J Micromech Microeng 14:604–611
34. Galambos P, Forster F (1998) An optical micro-fluidic viscometer. In: Proceedings of the ASME international mechanical engineering congress and exposition, Anaheim, California, November 1988, pp 187–191
35. Stiles PJ, Fletcher DF (2004) Hydrodynamic control of the interface between two liquids flowing through a horizontal or vertical microchannel. Lab Chip 4:121–124
36. Gaskell DR (1995) Introduction to thermodynamics of materials, 3rd edn. Taylor and Francis, London
37. Bassi FA, Arcovito G, D'Abramo G (1977) An improved optical method of obtaining the mutual diffusion coefficient from the refractive index gradient profile. J Phys E Sci Instrum 10:249–253
38. Timmermans J (1960) The physio-chemical constants of binary systems in concentrated solution. Interscience, New York
39. Einstein A (1956) Investigation on the theory of the Brownian movement. Dover, New York